CONF-800806--4

LA-UR-80-1494

TITLE: THE REVERSED-FIELD PINCH FUSION REACTOR*

MASTER

AUTHOR(S): R.L. Hagenson *Science Applications Inc.
Ames, Iowa 50010

R.A. Krakowski CTR-12 MS 641

SUBMITTED TO: 15th Intersociety Conversion Engineering Conference
Seattle, Washington, August 18-22, 1980

University of California

LOS ALAMOS SCIENTIFIC LABORATORY
Post Office Box 1663 Los Alamos, New Mexico 87545
An Affirmative Action/Equal Opportunity Employer

Form No. 836 R3
St. No. 2629
12/78

UNITED STATES
DEPARTMENT OF ENERGY
CONTRACT W-7405-ENG-36

THE REVERSED-FIELD PINCH FUSION REACTOR*

R. L. Hagenson
Science Applications, Inc.
Ames, Iowa 50010

and

R. A. Krakowski
University of California
Los Alamos Scientific Laboratory
Los Alamos, New Mexico 87545

Abstract

A conceptual engineering design of a fusion reactor based on plasma confinement in a toroidal Reversed-Field Pinch (RFP) configuration is described. The plasma is ohmically ignited by toroidal plasma currents which also inherently provide the confining magnetic fields in a toroidal chamber having major and minor radii of 13.7 and 1.5 m, respectively. The DT plasma ignites in 2-3 s and undergoes a transient, unrecycled burn at 10-20 keV for ~ 20 s to give a DT burnup of ~ 50%. The 5-s dwell period between burn pulses for plasma quench and refueling allows steady-state operation of all thermal systems outside the first wall; no auxiliary thermal capacity is required. Tritium breeding occurs in a granular Li_2O blanket which is packed around an array of radially oriented water/steam coolant tubes. The slightly superheated steam emerging from this blanket directly drives a turbine that produces electrical power at an efficiency of 30%. A borated-water shield is located immediately outside the thermal blanket to protect the superconducting magnet coils. Both the superconducting poloidal and toroidal field coils are energized by homopolar motor/generators. Accounting for all major energy sinks yields a cost-optimized system with a recirculating power fraction of 0.17; the power output is 750 MWe(net).

I. Introduction

The conceptual Reversed-Field Pinch Reactor (RFPR) study[1] has emphasized the development and evaluation of a realistic reactor-plasma model; an extensive parameter study based on this model has focused on a system with minimum power cost. Two major priorities and/or constraints are imposed. First, the engineering systems uses only conventional technology when possible, and, secondly, the ease of plant maintenance is stressed. The first-wall/blanket consists of a water-cooled copper and stainless-steel structure, with tritium breeding occurring in a granular-Li_2O packed bed. A direct-cycle, low-superheat steam system is proposed, thereby eliminating an expensive secondary coolant loop. Ohmic heating of the DT plasma to ignition is inherently made possible by the RFP confinement scheme. A batch-burn (unrecycled) operation is also chosen to eliminate advanced ash/impurity control (divertors) and fueling systems, although steady-state operation is not necessarily precluded by the RFP approach. The pulsed superconducting magnets and the associated energy storage system represent developmental items, although the magnet coils per se nearly meet state-of-the-art requirements (maximum field level ~ 2 T, maximum field rate-of-change ~ 40 T/s). Detailed designs exist for the proposed homopolar generators that energize the magnet systems; the homopolar generators could be replaced by ac machinery or fast-discharge dc alternators if these latter technologies prove to be economically attractive. Ease of maintenance is promised by designing for the vertical removal of the reactor core modules by means of a remote maintenance unit located within a common vacuum tunnel without disturbing the superconducting magnets. Confinement scaling for the RFP is independent of toroidal aspect ratio, allowing a mechanically open structure and a more easily maintained system.

This paper stresses equally the physics and engineering aspects of the RFPR design study. After describing the unique physical principles of the RFP in Sec. II, these principles are applied in Sec. III as the physical basis used to simulate the plasma burn and to estimate the overall reactor performance. The projected reactor engineering and technology are described in Sec. IV, which first addresses the plant operation and maintenance (Sec. IV.A) and subsequently summarizes major reactor subsystems (Sec. IV.B.).

II. Physical Principles

Like the tokamak, the RFP is a toroidal, axisymmetric confinement device. Both systems used a combination of poloidal, B_θ, and toroidal, B_ϕ, magnetic fields to confine a plasma in a minimum energy state. The poloidal field for both systems is created by inducing through transformer action a toroidal current, I_ϕ, within the plasma column; the toroidal field is created by external coils. Figure 1 compares the radial field and pressure profiles for both the RFP and tokamak systems. Toroidal equilibrium can be provided by either a conducting shell located near the plasma, an external vertical field or a combination of both schemes. The RFP requires a conducting shell for plasma stabilization against unstable magnetohydrodynamic (MHD) modes with wavelengths in excess of the shell radius, r_w, whereas the tokamak may not necessarily be subjected to this requirement. Localized MHD modes in the RFP are suppressed by the strongly sheared magnetic fields caused by a slight reversal of the toroidal field at the plasma edge. Although the tokamak may not require a conducting shell near the plasma column, avoidance of the kink instability establishes specific requirements on the relative magnitude of B_θ, B_ϕ, the plasma radius, r_p, and the major radius of the torus, R. Specifically, for the

* Work performed under the auspices of the US Department of Energy, Office of Fusion Energy.

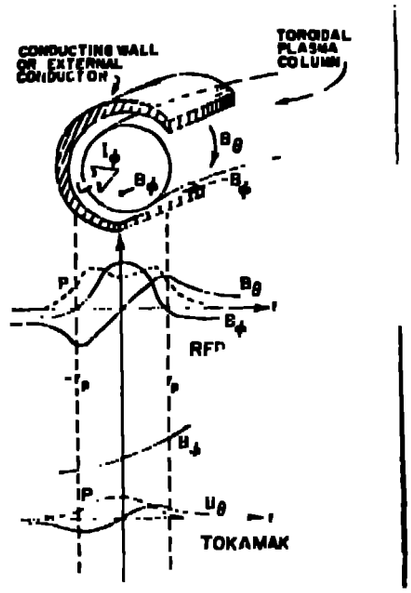

Fig. 1. Comparison of magnetic and pressure profiles for a dq/dr ≠ 0 stabilized RFP and a q > 1 stabilized tokamak.

tokamak the parameter $q = (r_p/R)(B_\phi/B_\theta)$ must be greater than unity. The criterion q > 1 assures that MHD kink modes with wavelengths in excess of the major circumference will be stable. Experimental values of q ≈ 2-4 at the plasma edge are required for stable tokamak operation. On the other hand, the RFP operates with q less than unity, q actually falling through zero and becoming negative outside the plasma region. The presence of a passive conducting shell replaces the q > 1 stability criterion with one that requires (dq/dr) ≠ 0; that is, the variation of the plasma/field shear should not exhibit a minimum in the region enclosed by the conducting shell. The reactor disadvantages associated with (passive) wall stabilization or (active) coil stabilization are countered by the advantages the RFP approach exhibits when not constrained by the q > 1 criterion. Imposition of the q > 1 constraint implies small values of R/r_p and B_ϕ/B_θ, which in turn create the following problems:

- Since the plasma pressure is essentially held by the poloidal field, the ratio of plasma pressure to total field pressure (i.e., the β parameter) is small, implying underutilization of magnetic field energy per unit of fusion yield.

- Since B_ϕ/B_θ is limited and since practical coil designs establish physical limits on the toroidal field, the plasma current I_ϕ is limited. This limit on I_ϕ generally precludes significant ohmic heating, thereby necessitating more complex and less efficient plasma heating schemes.

- The constraint that q > 1 also leads to limits on the plasma aspect ratio, R/r_p. In addition to engineering and system design constraints that accompany low-aspect-ratio toroids, relatively large inhomogeneities in the toroidal field result that in turn may lead to trapped-particle instabilities and enhanced transport of particles and/or energy.

- Generally, the q > 1 constraint drives the reactor design to utilize the highest possible toroidal fields and, therefore, leads to a more difficult magnet design and the storage of larger amounts of magnetic energy per unit of contained plasma energy (related to the aforementioned β issue).

The RFP approach essentially "differentiates away" the q > 1 constraint imposed on tokamaks and in its place requires dq/dr ≠ 0. The positive implications of the RFP stability criterion are:

- The aspect ratio R/r_p can be chosen solely on the basis of engineering considerations and convenience (i.e., desired power output and related economic considerations).

- The β limits predicted for the RFP are at least 10 to 50 times greater than q > 1 systems if ideal MHD theories are used. The predictions of resistive MHD theories reduce this factor to the range 3-10.

- The plasma may be ignited by ohmic heating alone.

- The confinement of high-to-moderate β plasma is achieved primarily by poloidal fields, which characteristically decrease with increased distance from the plasma, thereby reducing fields and stresses at the magnets.

- The use of highly sheared fields near the plasma edge for the RFP configuration makes possible a "vacuum" (low current) region between the plasma and first wall.

Although implications of these RFP characteristics are significant from a technological viewpoint, these benefits are accompanied by the need for a passively conducting first wall. Additionally, the energy that must be expended in establishing and maintaining the near minimum-energy RFP plasma is not known, but if this setup/maintenance energy is significant, operation as an ohmically-heated ignition device is made more difficult. Lastly, little or no consideration has been given by this study to the physics implications of fueling and ash removal systems required for a steady-state operation; the RFPR design presented here is based on a long-pulsed (~10 s) batch-burn operation. The favorable energy balance (recirculating power fraction is 0.17) computed for the batch-burn mode of operation reflects an efficient use of magnetic field energy that is characteristic of the RFP; technological issues associated with pulsed superconducting magnets and energy transfer/storage systems, however, require further development and study.

Stable field profiles within the plasma, an example of which is illustrated in Fig. 2, are modeled by Bessel functions. These profiles are integrated over the plasma radius to give the time-dependent, point-plasma model used in this study. Generally profiles that are stable according to ideal-MHD theories have been found numerically if the following three constraints are imposed:

- net positive toroidal flux: $\int_0^{r_w} B_\phi 2\pi r dr > 0$ (1)
- poloidal β limit: $\beta_\theta < 0.5 + B_\eta(B_\phi = 0)$ (2)
- Suydam criterion: $r^2[(d\ell n\nu/dr)]^2 + [dp/dr]^2\mu_0/B_\phi^2 > 0$, (3)

where $B_\eta(B_\phi = 0)$ is the local β at the zero point of the toroidal field, p is the plasma pressure and $d\ell n\nu/dr$ is the magnetic field shear, θ, with $\nu = B_\eta/rB_\phi = 1/qR$. The first two conditions are imposed on all RFPR burn conditions, whereas the third condition cannot be directly enforced because of the point model used. The Bessel function profiles, however, are a good approximation to profiles that satisfy the Suydam criterion.

The reactor computations assume field reversal occurs spontaneously and is maintained automatically throughout the burn period by plasma relaxation processes or instabilities. Self-reversal of the toroidal field is an experimental fact, but the associated energy loss is not known for large devices. The energy loss associated with this sustained self-reversal, therefore, was assumed equal to losses measured from large tokamak experimental energy confinement times equal approximately to 200 Bohm diffusion times, τ_{Bohm}). That self-reversal occurs is not in

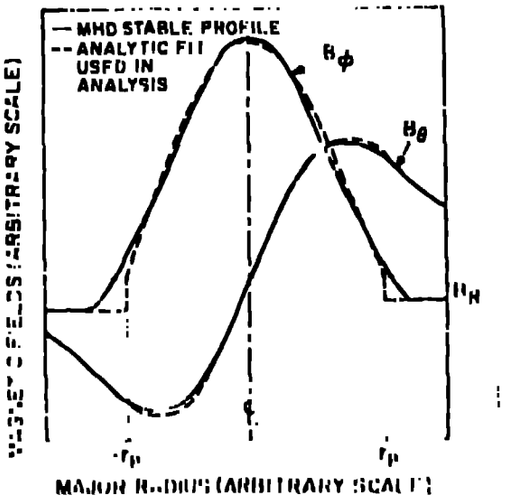

Fig. 2. Equation of stable RFP profiles computed numerically with the Bessel-function profiles used to generate the point RFPR plasma model.

question; the self-reversed state has been observed in many RFP experiments over the last 25 years. A recent theory[2] of relaxed states has lead to increased understanding of this minimum-energy, field-reversed state. Given any arbitrary dissipation mechanism, this theory predicts that a plasma surrounded by a flux conserving shell will relax to a minimum-energy state that is force-free with zero β. This minimum-energy state is described by the Bessel-function model given in Fig. 2. Numerical computations have confirmed this behavior for high-β, reversed-field plasmas. The key descriptive parameters in the Taylor theory[2] are the pinch parameter, Θ, and the reversal parameter, F, where

$$\Theta = B_\eta(r_w)/\langle B_\phi\rangle \quad (4)$$

$$F = B_\phi(r_w)/\langle B_\phi\rangle \quad (5)$$

$$\langle B_\phi\rangle = 1/r_w^2 \int_0^{r_w} B_\phi\, r dr \quad . \quad (6)$$

Figure 3 shows the locus of minimum energy states as described by the F - Θ diagram; both the analytic ($\beta = 0$) Taylor state and the numerical high-β states are shown. The desired field-reversed state corresponds to $F \leq 0$ and $1.2 < \Theta < 1.6$. High-β RFP states have been observed both experimentally and numerically for higher values of the parameter Θ, but the Taylor theory predicts an ultimate relaxation to the minimum energy states given on Fig. 3. It is noted that the minimum-energy tokamak state is described by the Taylor theory as the point where $F = 1$ for which $\Theta = r_p/R$. It has been assumed in modeling the RFPR that minimization of energy loss incurred during the field reversal would occur if the burn trajectory followed closely the F=0 curve or its high-β counterpart (Fig. 3). All RFPR burn trajectories adopted for this study closely track this locus of minimum-energy states.

Fig. 3. Region of stable minimum-energy states displayed on a F-Θ diagram for low-β (Taylor) and high-β (numerical) RFP plasmas.

III. Plasma Burn and Reactor Design Points

This section summarizes the physics models and computational results used to describe reactor startup, thermonuclear burn and postburn plasma quench. The design presented herein is based on a profile-averaged, zero-dimensional (point) plasma model. The poloidal and toroidal magnetic-field profiles within the plasma are described by the Bessel functions $A_\theta J_1(ar)$ and $A_\phi J_0(ar)$, respectively, which according to Fig. 2 show good agreement with calculated MHD-stable profiles. The constants A_θ and A_ϕ are determined by the conservation of total current and flux within the plasma column. Enforcing pressure balance and integrating over the isothermal plasma cross-section results in the spatially-averaged parameters used for the calculation of burn dynamics. A numerical calculation of the multi-species plasma (ions, electrons, and alpha particles) follows the plasma radius (i.e., field reversal point) with time in conjunction with the voltages and currents in both the plasma and associated electrical circuitry. Alpha-particle thermalization using a Fokker-Planck formalism, ohmic heating using classical resistivity, radiation (Bremsstrahlung, cyclotron, and line) losses, and anomalous (radial) thermal conduction and particle diffusion are included in this time-dependent model. As part of a continuing parametric analysis and refinement of the RFPR concept, a more realistic one-dimensional (radial) plasma model has been developed and applied[4] to the point design reported herein. The results of this comparison and possible alterations in future RFPR design points are also discussed.

A. Design Point Determination

An optimal burn cycle for the RFPR is one in which the plasma ohmically heats to ignition (5–6 keV), alpha-particle heating increases the plasma temperature to 10–20 keV and transport losses subsequently maintain a thermally stable burn until either a significant fuel burnup occurs or the maintenance of a steady-state burn in a fueled system is permitted. All investigations of burn cycles are based on batch operation in which the initial DT charge is partially burned, quenched and flushed from the system in preparation for a subsequent burn cycle. This procedure circumvents the need for both divertors for impurity/ash removal and the injection of fuel during the burn. Reduced or eliminated pulsed-power requirements, leading to a higher engineering Q-value, Q_E, lower costs and reduced thermal cycling of the first wall, make the steady-state option attractive, however, and warrant further study.

The startup time is taken as 10^{-3} of the energy containment time, which is estimated to be valid for a reactor plasma. A conducting copper first wall, with an electrical skin depth equal to the startup time, stabilizes the plasma and promotes field reversal during the Ohmic startup phase. An initially uniform toroidal field, B_{ϕ_0}, is superposed onto an increasing toroidal plasma current and results in a field configuration that is similar to a tokamak. This initially metastabilized system (i.e., $q > 1$) must be transformed into a high-β RFP configuration by proper field programming, self-reversal of the magnetic fields or a combination thereof (i.e., assisted self-reversal). Stability and quiescence during this setup phase seems unlikely, and turbulence similar to or greater than that exhibited in tokamaks may result. Energy losses incurred during this startup are not known and have not been explicitly included.

Burn cycles were adopted that operate near the minimum-energy plasma state, as defined by Taylor[2], and beta limits established by resistive MHD calculations[5–7] were enforced. Operating near the RFP minimum-energy state requires[2] $\theta = 1.5$–2.0 and $F = -1.0$. Maximum poloidal betas of 0.35–0.40 are inferred from resistive-MHD stability calculations. Transport scaling for RFP plasmas is unknown, although use of accepted tokamak scaling[8–10] gives an anomalous electron thermal conduction with an energy confinement time $\tau_E \approx 200\ \tau_{Bohm}$.[11] Anomalous transport would be caused by local instabilities and may be the result of pressure-driven modes, such as the resistive g-mode. As β_θ is increased transport would be enhanced, and a poloidal-beta limit at which the burn temperature would saturate results, yielding thermal stability. The use of an enhanced loss given by $\tau_E = 200\ \tau_{Bohm}$ or a loss mechanism that is driven explicitly by a limiting beta[12] give similar results for reactor sizes of economic interest ($r_w = 1$–2 m).

A typical burn trajectory for the RFPR is shown in Fig. 4 using $\tau_E = 200\ \tau_{Bohm}$ as the anomalous energy loss time. A thermally stable burn results at a nearly optimal temperature of 10–20 keV, resulting in a fuel burnup, $f_B \approx 0.5$. A poloidal beta of ≈ 0.4 is reached during the burn, which is ultimately terminated as fuel burnup and

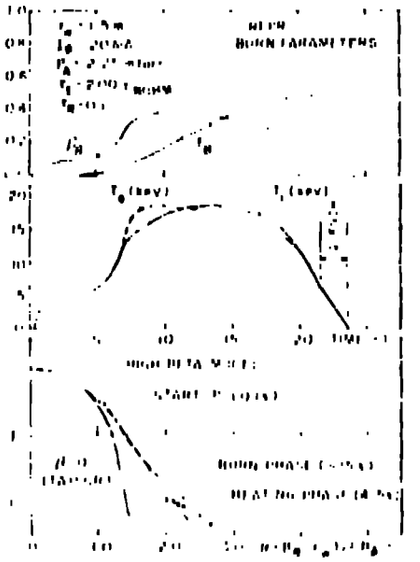

Fig. 4. RFPR (superconducting coils, discrete system) burn parameters using an energy confinement time $\tau_E = 200\ \tau_{Bohm}$. The burn trajectory is in good agreement with that computed by the hybrid model for a minimum-energy configuration.[4]

alpha-particle buildup cause the ion temperature to fall below 8 keV. A similar trajectory is produced using an anomalous loss rate dictated by a limiting beta.[12] In either case the burn trajectory is in good agreement with that suggested by the high-β model[3] for a minimum-energy configuration.

The burn trajectory shown in Fig. 4 is used as the reference case for evaluation of reactor performance. This thermally stable burn achieves ignition in ~ 3 s. The ~ 15-s batch burn is followed by a 2-3 s quench period during which time the trapped magnetic field and post-burn plasma would be thermally dissipated at the first wall. Flushing the system with neutral gas, while continuously evacuating the alpha-particle ash, readies the chamber for the subsequent burn cycle. The burn cycle is sustained for 21.6 s, and 5 s is allowed for evacuation and refueling; the total cycle would be 26.6 s.

Termination of the burn occurs as the toroidal current is decreased sinusoidally by the external circuitry, allowing the plasma to relax to the wall. The plasma would then be confined by the first wall, where heat loss is controlled by radiative processes and thermal conduction across magnetic field trapped inside the plasma. The introduction of neutral gas[13] during the quench period should permit efficient energy removal in the desired time. All of the field trapped inside the plasma at quench is conservatively postulated to be thermally dissipated at the first wall. Employing a controlled rundown in which the plasma current is decreased as the plasma edge cools may allow a large fraction of the trapped field to be released and recovered. Since ~ 40% of the recirculating electric power is required to replace this dissipated field energy, significant increases in the engineering Q-value will occur if a portion of this quench field is recovered.

B. One-Dimensional Plasma Simulations

A comparison with the one-dimensional (radial) MHD model is used to gauge the predictions of the point model.[4] Establishing a 14.1-MeV neutron wall loading near the reference design[1] (2.7 MW/m^2), while simultaneously maintaining a similar power output, fixes the plasma line density at $1.5(10)^{21}$ m^{-1}. A plot of the plasma Q-value, Q_p, versus the initial bias magnetic field on axis, $B_{\phi 0}$, is shown in Fig. 5, which illustrates that the Q-value increases as $B_{\phi 0}$ decreases because of the reduced quantity of magnetic field remaining to be resistively dissipated in the post-burn plasma. If $B_{\phi 0}$ is reduced below ~ 5.8 T, plasma ignition is not possible. A comparison between the optimized point-model calculation and the one-dimensional optimized calculation is shown in Table I. As noted in Fig. 5, the poloidal beta increases from 0.11 to 0.51 as the magnetic fields are reduced. Although high, this beta remains within stability limits predicted by ideal MHD theory. If lower beta limits are enforced, the decrease in system performance and increased unit cost does not become serious until the maximum allowable β_θ falls below 0.15. The time-dependent electron and ion temperatures for the Q_p = 20.4 case shown in Fig. 4 are plotted in Fig. 6 along with the fractional burnup and poloidal beta. The total power computed by the one-dimensional simulation

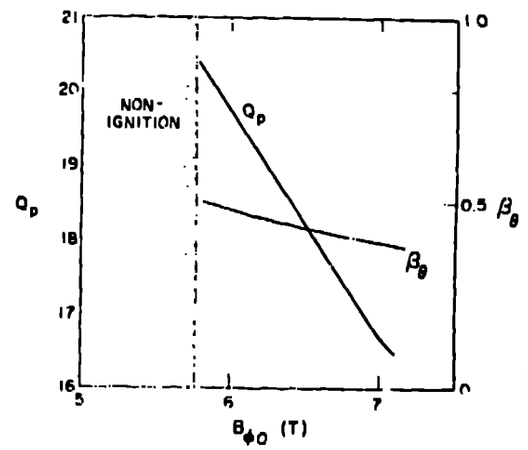

Fig. 5. Dependence of plasma Q-value and associated maximum poloidal beta on the initial toroidal bias field.

is within 5% of that determined by the zero-dimensional model (Table I).

IV. Reactor Engineering and Technology

The physics principles described in Sec. II and the burn simulations described in Sec. III have been combined in a parametric study to give a cost-optimized design point by which key engineering and technological issues could be examined. Table II gives a summary description of key reactor parameters that have emerged from this study. A parallel but independent, reactor study[14-15] yields plasma characteristics and reactor performance close to those reported here.

A. Description of Plant Operation and Maintenance

The RFPR design presented here would operate as an unrefueled (batch-burn) system in which preionization, field reversal and ignition by ohmic heating would occur in a run-up period t_{ru} ~ 0.1 s. The transient burn would occur for t_b = 21.6 s in a 12.7-m major radius torus with a first-wall radius equal to 1.5 m. Approximately 50% of the DT fuel would be consumed, yielding a total thermal energy each pulse of 2048 GJ (1000 MWt average thermal power) and an average neutron wall current of 2.7 MW/m^2. The recirculating power fraction for the 750-MWe(net) plant would be ϵ = 1/Q_p = 0.17.

The long-pulsed operation is depicted by Fig. 7 in terms of the poloidal field coil (PFC) current, I_{pc}, the toroidal plasma current, I_p, and the toroidal fields, B_ϕ (initial) and $-B_\phi$(reversed). The toroidal field coil (TFC) is first energized to produce a uniform toroidal bias field $B_{\phi 0}$ = 5.6 T. At this time the plasma is preionized, and a constant current, I_{pc} = 1.9 MA, is flowing in the PFC. The PFC current is reversed in the presence of the low-temperature but electrically conducting plasma by switching the PFC energy temporarily to a homopolar motor/generator (a capacitive element) and then

Table I
Summary Comparison of Energy Balance for Zero- and One-Dimensional Burn Models

Parameter (MJ/m)	Zero-Dimensional Burn	One-Dimensional Burn (Optimized)
Burn time (s)	21.6	22.
Initial plasma energy	0.05	1.0
Final plasma energy	2.5	3.7
Radiation energy[a]	28.1	19.3
Ohmic heating energy	7.1	8.9
Plasma energy loss (conduction)	147.5[b]	146.7
Plasma expansion energy	0.7	0.0
Eddy current losses in the blanket/shield	1.5	---
Magnetic-field energy inside first wall at end of burn cycle	51.6[c]	30.6
Magnetic-field energy transfer losses	8.1[d]	---
Fusion neutron energy (14.1 MeV)	676.5	646.2
Auxiliary/neutron energy requirements	14.3[e]	---
Q_p = (fusion energy)/(Ohmic + field energy)	14.4	20.4

[a] Bremsstrahlung and line radiation.

[b] based on an energy confinement time equal to 200 Bohm diffusion times.

[c] A significant fraction of this energy would be recovered during plasma current rundown and quench (~ 50% recovery in RFPR reactor design).

[d] based on a 95% efficient inductive/capacitive transfer from the homopolar motor/generator (capacitive) to and from the magnets.

[e] the cryogenic system required for the superconducting magnets consumes 21% of the auxiliary power.

Fig. 6. Time dependence of average plasma temperatures, beta and % fuel burnup fraction for the optimum design point.

back to the PFC in the time $t_R \approx 0.1$ s. The homopolar motor/generator acts only as a transfer element, in that the PFC energy (11.0 GJ) resides for most of the time in the superconducting coils. Upon reversal of the PFC current, a plasma current is induced during the time when the toroidal field continues to reconnect inductively. A homopolar motor/generator is also used as the main energy store (3.7 GJ) for the TFC system. The toroidal field ultimately reverses in the vacuum/blanket/shield region between the PFC and the plasma edge, the B_ϕ field within the highly-conducting plasma being trapped and remaining positive. When toroidal field is fully reversed outside the plasma at a value $-B_\theta$ and the plasma current has reached a maximum, both PFC and TFC systems are "crowbarred" (i.e., the homopolars are short-circuited from the coils). Both I_ϕ and $-B_\theta$ are maintained constant throughout the burn period, t_B, by a self-reversal mechanism that is characterized by an energy confinement time $\tau_E \approx 200\ \tau_{Bohm}$. Figure 4 depicts the time dependence of ion and electron temperatures, poloidal beta and fractional burnup. The burn phase is terminated when the ion temperature

Table II
Summary Description of RFPR Design Parameters

Parameter	Value
First-wall radius, r_w(m)	1.5
Major radius, R(m)	12.7
Toroidal plasma current, I_ϕ(MA)	20.0
Toroidal field at the coil, $B_{\phi c}$(T)	2.0
Poloidal field at the coil, $B_{\theta c}$(T)	2.0
Toroidal coil energy, $W_{B\phi}$(GJ)	3.7
Poloidal coil energy, $W_{B\theta}$(GJ)	11.0
Field rise time, τ_R(s)	0.1
Burn time, τ_B(s)	21.6
Cycle time, τ_C(s)	26.6
Average fuel burnup, f_B	0.5
Average plasma density, $n(10^{20}/m^3)$	2.0
Average plasma temperature, $T_{i,e}$(keV)	15
14.1-MeV neutron current at first wall, I_w(MW/m^2)	2.7
Engineering Q-value, Q_E	5.8
Recirculating power fraction, $\epsilon = 1/Q_E$	0.17
Average blanket power density, P_{BLK}(MW/m^3)	4.7
Average system power density, P_{SYS}(MW/m^3)	0.9
Total thermal power, P_{TH}(MWt)	3000
Net electrical power, P_E(MWe)	750
Net plant efficiency, $\eta_p = \eta_{TH}(1-\epsilon)$	0.25

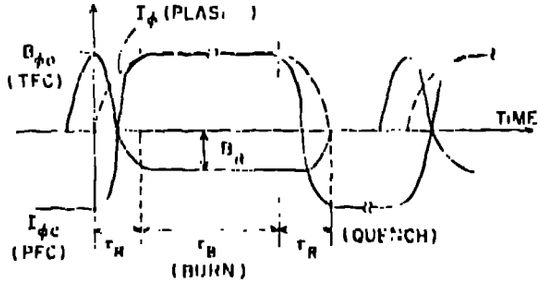

Fig. 7. Typical RFPR burn cycle depicted in terms of plasma current, poloidal coil current and toroidal field.

decreases below 8 keV because of fuel burn-up and alpha-particle accumulation. At this point in the RFPR power cycle the crowbar switches in both the TFC and PFC electrical circuits are opened. Using the homopolar motor/generator as a transfer element, the PFC current is again reversed, and the associated energy is stored in the superconducting PFC. The toroidal field energy not trapped in the plasma is also transferred to the homopolar motor/generator used for the TFC energy storage. All field energy trapped within the plasma is assumed to be thermally dissipated during the plasma quench. The coil/homopolar transfers occur with an intrinsic machine efficiency of 95%. Parametric studies[1] show that the reactor performance is not seriously degraded until this transfer efficiency falls below ~ 80%. Cooling of the postburn plasma now occurs. A quench process that is limited by classical thermal conduction and resistive field decay would be prohibitively long. Generally, it is supposed that neutral gas would be added to the plasma and instabilities would occur to aid in a timely and controllable plasma quench. The postburn plasma energy (2.5 MJ/m) and the associated trapped field energy, (21.5 MJ/m) amount to a total first-wall energy density of 2.53 MJ/m^2, which is assumed to be uniformly deposited on a ~ 4-s timescale. For ~ 5 s after initiating the plasma quench the continuously operating vacuum system would purge the 568-m^3 plasma chamber while fresh DT gas would be added. Typically, the baseline steady-state helium concentration would be maintained by this continuous purge at or below ~ 1 atom %. Figure 8 gives the time-dependence of important plasma powers computed for this design.

The power-plant embodiment that has been developed on the basis of this reactor operation is depicted in Figs. 9 - 13. The 1.5-m-radius plasma chamber is formed by 40, 2-m-long first-wall/blanket/shield modules, four of which are depicted in Fig. 10. Figure 11 gives an isometric view of the reactor, an elevation view is presented in Fig. 12 and Fig. 13 summarizes the

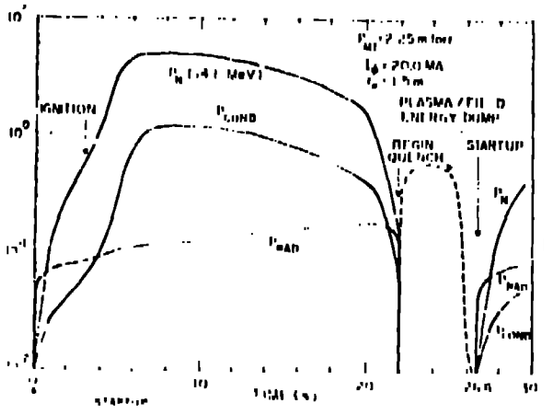

Fig. 8. Time dependence of neutron, P_N, conduction, P_{cond} and radiation, P_{RAD}, power flux at RFPR first wall. The power flux associated with the plasma/field dump is time-shrunk.

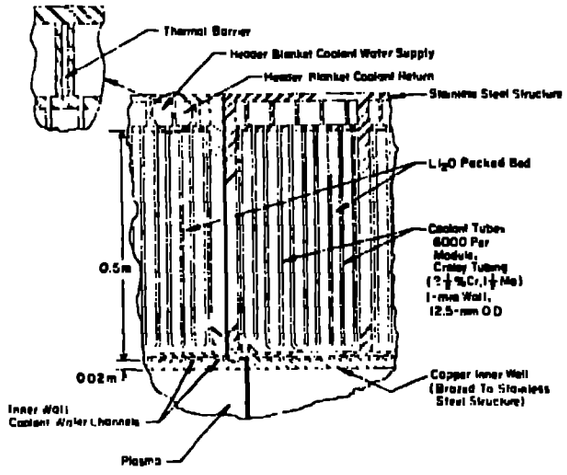

Fig. 9. Sectional view of steam-generating, packed bed blanket and first-wall assembly.

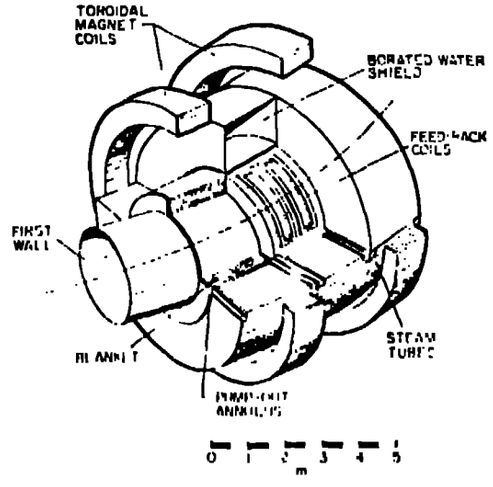

Fig. 10. Isometric view of four 2-m-long RFPR reactor modules including the copper first wall, Li_2O packed bed and associated high-pressure steam tubes, feedback coils, water shield and toroidal field coil.

major coolant flow for this system. The 1.2.7-m major-radius torus is constructed within a vacuum tunnel and is completely detached from the PFC system. A separate water-cooled copper first wall (20-cm thick) provides an electrically conducting shell and operates near the blanket temperature (520 K). The 0.4-m-thick stainless-steel blanket contains a 60 v/o Li_2O packed bed into which penetrate radially water/steam-cooled U-tubes (Fig. 9). A low-pressure (0.1-MPa) helium purge gas is drifted through the granular Li_2O bed to extract bred tritium. The slightly superheated (5-5) steam emerging from this blanket is used

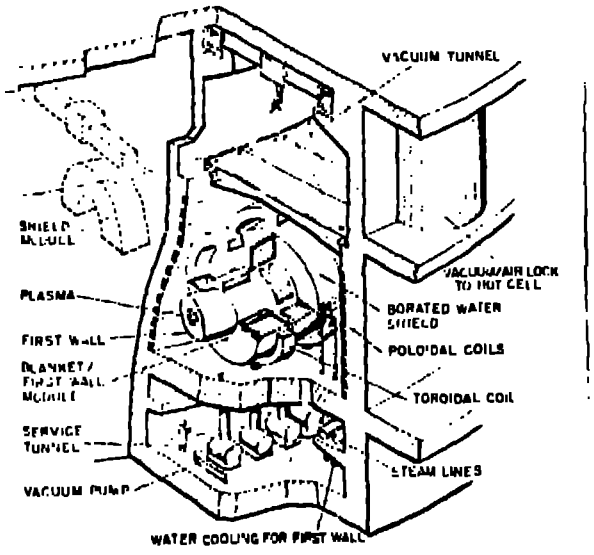

Fig. 11. Isometric view of RFPR power plant.

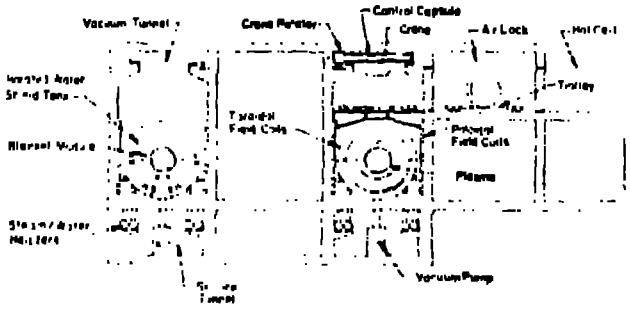

Fig. 12. Cross-sectional view of RFPR torus located in a vacuum tunnel.

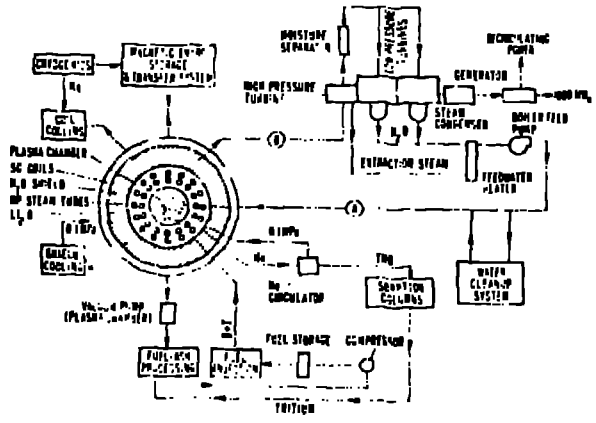

Fig. 13. Line diagram for all major subsystems needed for the direct-steam-cycle RFPR. Not shown is the separate first-wall coolant loop that would primarily serve reheat functions.

drive a turbogenerator directly, the first-wall water coolant being used only for feedwater and reheat functions. For the 81% duty factor characterizing the burn cycle depicted in Fig. 8, the intrinsic thermal capacity of this blanket configuration results in less than a 5-F temperature cycle within the blanket structure, although the averaged first-wall temperature undergoes a 28-F excursion.

The water-cooled blanket adopted by this design was projected to be inherently more economical than designs using flowing, liquid metal or high-pressure helium coolants. Conservatively limiting the copper first-wall coolant temperature to 300 K, however, required a separate water-coolant loop which could be used only for feedwater heating (not shown in Fig. 13). Since 14% of the total thermal power is removed by the first-wall coolant circuit, including the plasma/field energy dump and all alpha-particle energy, the overall thermal-conversion efficiency is computed to be only 38%, compared to 40% for a comparable light-water-cooled fission reactor. Parametric studies show[1] that operating the first wall at the blanket coolant temperatures would increase the overall cycle efficiency to 29%. Increasing the blanket/first-wall coolant temperature by 100 K above the values reported in Table III would result in a 35% cycle efficiency. Higher temperature operation, however, would require a reassessment of the use of conventional blanket materials.

An important objective of the preliminary plant layout depicted in Figs. 11 and 12 is to quantify the reactor maintenance procedure. Additionally, the preliminary plant layout is useful for estimates of plant capital and power costs, which are summarized in Ref. 1. As depicted in Figs. 11 and 12, the two major coil systems that drive the RFPR would be permanently fixed. The PFC system would consist of large,

Table III
Summary of Key Neutronic and Thermohydraulic Parameters

Parameter	Value	
Tritium breeding ratio	1.11	
Nuclear heating in the blanket (MW/m)	21.1	
Nuclear heating in the shield (MW/m)	0.36	
Total energy deposited into first wall (MW/m)	14.1	
Total rated power (MWt/MWe)	3000/750	
System pressure (MPa)	5.5	
	First Wall	Blanket
Coolant flow rate (kg/s)(a)	40.6	29.7
Inlet temperature (K)	460	383
Outlet temperature (K)	540	551

(a) per module, 40 modules comprise the reactor.

superconductors (NbTi/Cu/stainless-steel) that encircle the inner and outer major radii of the reactor. The PFC system would be permanently fixed to structure associated with the walls of the toroidal vacuum tunnel and would not interfere with procedures needed to remove any of the 40, 2-m-long modules. The TFC system consists of twenty low-field (2.0-T) circular coils that are positioned over alternate reactor modules; each NbTi/Cu/stainless-steel TFC would have a 3.6-m radius, a 1.2-m length and 0.5-m thickness. The current distribution in the PFC system would assure that the vertical field component is sufficient to maintain the plasma in toroidal equilibrium. Small, normal-conducting feedback-stabilization coils would be placed between the blanket and shield (Fig. 10); these slow-pulsed coils (< 10-Hz) are considered part of the reactor module assembly.

A number of vacuum entry schemes have been considered. One scheme uses a mobile remote-handling unit and life-support system that would be positioned over the reactor module(s) to be repositioned. The mobile remote-handling unit would be sized to contain only one replacement module. The unit would move in the reactor hall above the vacuum tunnel, would make a local vacuum seal and, after the unit was evacuated, would disconnect and remove a 4-m-wide by 8-m-long vacuum cover plate. Two toroidal field coils and approximately four reactor modules would be exposed and directly observable by maintenance personnel situated in a control room associated with the mobile replacement unit. An alternative scheme would simply bring the entire vacuum tunnel to atmospheric pressure (inert gas) and use only a mobile replacement control room to remove modules first to the reactor hall and ultimately to a staging/repair hot cell area (Figs. 11 and 12). In all likelihood both maintenance schemes might be used; the mobile replacement unit would be employed only for unscheduled maintenance, whereas the latter approach would be used during a major reactor overhaul. A third approach would operate both the vacuum tunnel and the reactor hall under vacuum; the vacuum building approach was not given detailed consideration. The method by which blanket and shield modules would be removed is depicted in Figs. 14 and 15. The PFC system is not shown, since it would not interfere with the module replacement operation. As noted previously, the TFC structure would be fixed and would be sufficiently open to permit removal of blanket/shield modules by simple translational and vertical motions. Each 2-m-long by 1.5-m-radius module would be hydraulically and electrically independent. As shown in Fig. 14, a 50-tonne hemi-cylindrical shield tank would be lifted between the stationary toroidal field coils, after draining approximately 25 tonnes of borated water. Three first-wall/blanket modules, each weighing 60 tonnes, would then be removed. The superconducting magnet coils are considered to be highly reliable components that would rarely need maintenance. Provisions are made, however, for unexpected outages in these coils. Replacement of a TFC would require a number of blanket/shield modules to be removed, as described above. In addition a lower hemi-cylindrical shield segment would be extracted from the vacuum tunnel before the TFC (~ 70 tonnes) could be lifted from the reactor assembly. All poloidal field coils in

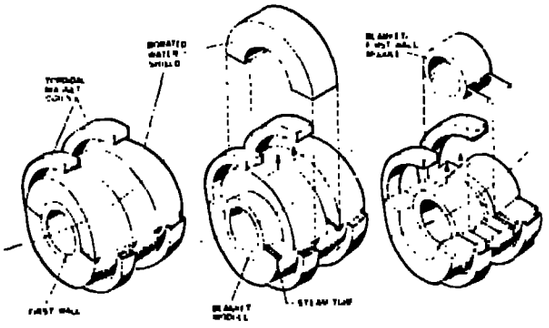

Fig. 14. Schematic drawing of RFPR modules, illustrating removal sequence of shield and first-wall of shield modules.

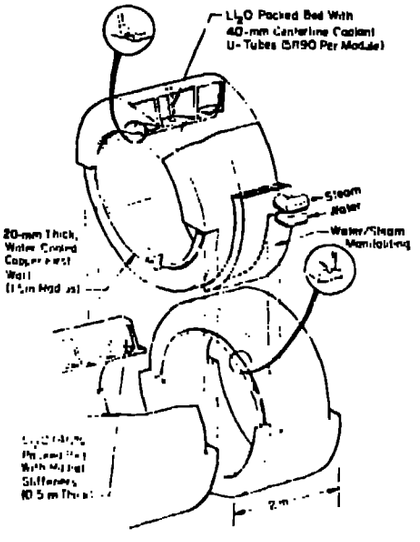

Fig. 15. Isometric view of reactor module illustrating replacement scheme.

principle would be directly accessible in segments for maintenance without disturbing the reactor torus or the vacuum tunnel.

Analysis of the remote handling task has not progressed beyond the level of the foregoing description. Given highly reliable PFC and TFC systems, each of the 40 reactor modules would require approximately 4-6 disconnections: two high-pressure (5.5 MPa, ~ 150-mm diameter) steam lines, two high-pressure water lines (5.5 MPa, ~ 100-mm diameter) and electrical connections to the slow feedback coils. The power density in the borated-water shield would be very low (0.02 of the fusion energy, 10 kW/m^3) and could be removed by natural convection and conduction to the room-temperature support structure. Mechanical

and reliability analyses of this joining/disconnection requirement remain to be performed.

B. Reactor Subsystems

This long-pulsed RFPR design invokes a conventional, steam-generating technology embodied in the water/steam cooling of a packed Li_2O bed, stainless-steel structure and stagnant borated-water shield. The direct-cycle steam system is not uniquely applicable to the RFPR, but adaptation of this scheme was made to investigate the technological and economic tradeoffs associated with the elimination of a secondary heat-transfer loop. This section addresses neutronic, thermohydraulic and mechanical design of the blanket. Tritium handling, vacuum system requirements, energy storage and switching, and superconducting magnet coil requirements are also briefly described. Reference 1 provides a more detailed treatment of these subsystems.

1. Neutronics Analysis. Two sub-modules constitute the RFPR core; the first-wall/blanket module and the shield module. The first-wall/blanket module consists of a plasma-vacuum region followed by a 20-mm-thick copper first wall. Use of a copper first wall represents a net benefit for tritium breeding by enhancing the neutron multiplication. The blanket is comprised of a water/steam-cooled packed Li_2O bed and stainless-steel structure (40 v/o Li_2O, 10 v/o H_2O, 15 v/o steel, 35 v/o void). For the purpose of the neutronics analysis all materials in the blanket were homogenized. The shield module consists of a 0.1-m-thick Cu feedback coil, a 0.1-m-thick lead region for gamma-ray attenuation and a stagnant 1.5-m-thick borated-water (18.0 v/o ^{10}B) shield. Beyond the shielding are located the Cu/NbTi magnets.

For a 14.1-MeV neutron wall loading of 2.7 MW/m^2 the total heating in the first-wall/blanket module is 28.2 MW/m, with an average power density in the blanket of 5.1 MW/m^3. The first-wall/blanket system recovers 79.1% of the fusion neutron energy. The tritium breeding ratio is 1.11 with a total neutron energy worth of 16.3 MeV. The ability to breed tritium without a neutron multiplier results from the 14.5% neutron multiplication through the (n,2n) reaction in the copper first wall.

2. First-Wall and Blanket Thermohydraulics. The 20-mm-thick copper first wall receives 38% of the total thermal energy produced by the reactor. This first-wall thermal loading is much greater for the RFPR than for an equivalent tokamak because of the assumed batch-burn, divertorless operation. In addition, the higher Bremsstrahlung flux, wall thickness and (n,2n) reaction rate account for the greater first-wall thermal fluxes and power densities. Table IV summarizes the various thermal inputs to the first wall. One manifestation of the (n,2n) reaction in copper can be observed by comparing the volumetric heating rate with that in the stainless steel structure. The first-wall energy flux resulting from the shorter-time deposition of plasma/field energy during the quench period is approximately equal to the Bremsstrahlung and thermal conduction fluxes encountered during the burn period. Consequently, the first-wall thermal flux remains relatively

Table IV
Summary of First-Wall Thermohydraulics

Parameter	Value
Water flow rate (kg/s)	1584
Inlet pressure (MPa)	5.52
Inlet temperature (K)	360
Outlet temperature (K)	530
Number of coolant channels/module	100
Coolant channel cross-section (mm × mm)	15 x 15
Coolant channel length (m)	9.4
Flow rate per channel (kg/s)	0.40
Flow velocity (m/s)	2.07
Reynolds number	176,000
Peak heat flux at channel wall (MW/m^2)	
• Local	1.79
• Averaged	1.12
Volumetric nuclear heating rate in copper averaged over burn time (MW/m^3)	33.8
Averaged surface heat flux (MW/m^2)	
• During burn	0.86
• During 4-s quench	0.64
Peak wall temperature at coolant channel (K)	552
Maximum copper temperature (K)	613
Maximum steel temperature (K)	584

constant over the entire power cycle for the assumed 4-s quench period.

The maximum change in the averaged first-wall temperature is 28 K, and at the plasma/first-wall interface the temperature change amounts to 68.5 K. The maximum temperature change in the stainless-steel structure immediately behind the copper first-wall during a given burn cycle is 21 K. Because of the moderate temperature change during a burn cycle, thermal fatigue should not be serious for the proposed high-strength copper alloy.[16] The issue of radiation effects and the related synergism associated with this thermal cycling, however, requires further study. It is emphasized that the copper first wall does not serve a structural or vacuum-barrier function other than the requirement to preserve its self-integrity and to maintain an acceptable electrical resistivity.

The spacing between the adjacent coolant tubes in the packed-bed blanket (Fig. 9) was made small in order to minimize the temperature extremes in the packed bed. The heating rates vary by a factor of 9 from the first-wall region to the outer blanket region, and the average power density is 5.1 MW/m^3. The radial coolant U-tubes, (Fig. 9) are spaced on a uniform rectangular grid, projecting radially inward from the outboard manifolds. Because of the cylindrical geometry, the spacing between adjacent U-tubes increases with radius from 40-mm near the first-wall region to 50-mm in the outer blanket region. Each leg of the U-tube is parallel with a center-to-center spacing of 40-mm. Nominally, 5890 U-tubes are required for each 3-m-long module. The tubes are made of Croloy 2-1/4 steel alloy with an outside diameter of 12.5-mm and a 1-mm wall thickness. Each coolant tube supports external fins arranged longitudinally to enhance heat transfer from the packed Li_2O bed. The results of the blanket thermohydraulic calculations are summarized in Table V. The maximum temperature change for a U-tube during a power pulse amounts to only 2.4 K.

Table V
Results From Blanket Thermohydraulics Calculations

Parameter	Value
Coolant flow rate (kg/s)	788.4
Coolant flow rate per U-tube (kg/s)	$3.37(10)^{-3}$
Inlet temperature (K)	383
Outlet temperature (K)	551
Nominal coolant pressure (MPa)	5.5
Heat flux at U-tube inside diameter (MW/m^2)	0.43 - 0.066
Volumetric heating rate in packed bed (MW/m^3)	9.42 - 0.7
Coolant mass velocity ($kg/s\ m^2$)	38.9
Coolant Reynolds number	
• Water inlet	$4.74(10)^6$
• Steam outlet	22,000
U-tube pressure drop (kPa)	< 1.4
U-tube wall temperature (K)	475 - 781

Because of the large thermal capacity and low thermal diffusivity of the Li_2O powder, any auxiliary thermal storage to maintain a constant outlet coolant temperature appears unnecessary.

3. Tritium Handling. Tritium isolation from both the first-wall and blanket coolant loops has been assumed on the basis of present understanding. Low-levels of oxygen in the packed-bed, presumably present in reactor-grade helium or released by the destruction of Li_2O occurring during the breeding process, will rapidly oxidize gaseous T_2. Diffusion of T_2O through steel at the temperatures envisaged should be negligible. Isolation of tritium gas in the plasma chamber from the first-wall coolant water also appears feasible in that diffusion at the 613-K peak temperatures would in principle lead to negligible transport through the 20-mm-thick copper that separates the plasma chamber from the first-wall coolant channel. The tritium containment and isolation question, however, remains far from resolved for an actual engineering system (i.e., systems with joints, weldments, three-dimensional shapes, etc.). The maintenance of a tritium-free first-wall coolant is probably more uncertain than for the blanket coolant system. The separation of coolant loops, however, may permit operation of a slightly contaminated first-wall loop, if necessary, although the impact of this operational mode on the overall fuel balance remains to be quantified. Lastly, detailed parametric studies of the tritium release kinetics from the Li_2O packed bed have been made,[1] but the performance of tritium inventory issue remains to be accurately resolved.

4. Vacuum System. Roots blowers and cryopumps are considered as potential candidates for the primary vacuum system. Two-stage Roots pumps have high-pumping speed down to pressure of $\sim 10^{-2}$ torr with significant reduction in speed below that level. These robust rotary-pumps are well suited to maintaining 10^{-1} torr in large systems over long periods of time with little attention. Scaling these pumps to larger sizes, a 25,000 ℓ/s pump would be ~ 2.2 m in diameter by 1.8 m in length and consume ~ 150 kWe. Using one pump for each of 40 module gives a pumping capacity of 10^6 ℓ/s with a total power consumption of 6 MWe.

The outgassing rate from degreased steel has been taken as 10^{-3}–10^{-4} ℓ torr/s m^2, which for a total tunnel surface area of ~ 10^4 m^2 gives 1–10 ℓ torr/s and a minimum base pressure of 10^{-5}–10^{-6} torr for a total pump speed of 10^6 ℓ/s. Between each 2^{s}-s burn pulses the 560 m^3 plasma chamber is filled with DT to a pressure of ~ 10 mtorr, requiring a throughput of ~ 200 ℓ torr/s for which a minimum base pressure during reactor operation is $2(10)^{-4}$ torr.

Difficulties envisaged by using a Roots vacuum system are the relatively high base pressures and the presence of a background magnetic field that could interfere with a rotating machine. Use of cryopumps should alleviate both the base-pressure and magnetic-fields problems. A cryogenic system would be similar to that used for other fusion reactor designs.[17] One-half of the capacity would be used at any given time, allowing for pump regeneration without interception of the vacuum system. Using a cryogenic pumping speed for DT of $1.3(10)^3$/s m^2, the pumping capacity of the 1,600-m^2 system is 10^8 ℓ/s, which is 100 times that required for idealized RFPR operation. The pumping speed for helium is approximately 75% that of hydrogen, whereas air is pumped at ~ 5% the rate of hydrogen. Approximately 6.2 MWe of refrigeration power is needed to power this 10^8 ℓ/s cryogenic system.

5. Energy Transfer, Storage and Switching. Homopolar motor/generators are proposed to drive the toroidal and poloidal magnet coils. A detailed conceptual engineering design of a 1-GJ homopolar machine with a high-efficiency 30-ms discharge time has been made.[18] This machine has an active rotor length of ~ 13-m, 2-m-diameter rotors and spins at 277 m/s. The magnetic field is produced by superconducting Nb_3Sn magnets with a peak field of 8 T. This 95% efficient machine in many ways is beyond the state-of-the-art. The combination of surface speed and brush current density has not been achieved with solid brushes. Aluminum rotors are proposed for the first time, and this design would be the first pulsed homopolar to use superconductors. These problems arise only because of the lack of development effort rather than because of fundamental difficulties. A modest program should lead to a homopolar having good efficiency (> 90%) and economics (≤ 1¢/J). Parametric studies[1] show that the RFPR performance is not seriously degraded until this efficiency falls below ~ 80%.

Conventional switching is considered, with each closing switch consisting of a parallel-connected ignitron and a mechanical bypass switch; each opening switch would be constructed from a vacuum interrupter operating in parallel with a mechanical bypass switch [19–20]. The reliable operation of ~ 2,700 switches, each carrying 25 kA, is of primary concern and provides an impetus to develop larger switching elements (> 100 kA) with high energy transfer efficiency and reliability. The technology needed for these switches appears straightforward, but a development effort is required. Solid-state switches may always be invoked, although economic considerations warrant the development of efficient mechanical breakers.

6. Superconducting Magnets. Superconducting coils are used for both the poloidal and toroidal field systems. A maximum field at the coils of ~ 2.0 T gives a maximum field rate of change of 20-40 T/s for the 0.1-s startup. This rate-of-change and absolute magnitude of magnetic field represent near-term technology for NbTi superconductors. A detailed design of a 20 T/s coil with a maximum field of 7 T has been made.[21] Potential problems are encountered with the coupling of the toroidal coil to the poloidal system. The enhanced eddy-current losses induced in the toroidal coil can be greatly reduced by alternating the twist direction of the filaments as the coil is wound.

The arrangement of magnets in this design is unique and generally reflect the advantage of plasma confinement primarily by energy-efficient poloidal fields. Consequently, the poloidal field and vertical field coils are removed from the reactor core per se. The resulting increase in blanket and shield accessibility leads to operational and maintenance advantages that far outweigh the ~ 50% increase in stored magnetic energy. The bipolar operation of the poloidal coil system results in the homopolar motor/generator serving only as a capacitive transfer element. Homopolar motor/generators serve as an energy store for the toroidal field coils, which are adequately spaced within a 0.5% field-ripple criterion to allow blanket/shield replacement without disturbing these permanently-fixed magnets.

Small, normal feedback coils must be affixed to the inner radius of the shield sub-module. The slow (~ 10 Hz) feedback requirements, coil design, power supplies, and instrumentation/control systems have not been specified. Although preliminary estimates indicate acceptable energy consumption and technical feasibility, this important issue must be addressed in considerably more detail.

V. Conclusions

As for most conceptual fusion reactor studies, the credibility and feasibility of most engineering systems is determined in large part by the physics assumed to generate the reactor plasma model and related energy balances. Energy loss from the plasma incurred during initiation and sustenance of the field-reversed configuration represents the major uncertainty. The plasma/field/first-wall response during the rundown phase of the long-pulse power cycle presents a second important uncertainty. Within the constraints of the assumptions made for both energy containment and rundown processes, feasible technical designs for all engineering systems have been identified. Furthermore, sensitivity studies of the influence of key physics (i.e., beta) and engineering parameters (i.e., energy transfer/storage efficiency) indicate that a relatively safe margin for error exists before a serious degradation in RFPR system performance or cost is incurred.

In many ways the RFPR presents desirable system on which to examine the technical and economic feasibility of magnetic fusion power, given a favorable resolution of the above confined plasma issues. The results of this study indicate that an efficient power plant may emerge from the relatively low technology requirements embodied in cyclic heating and batch-burn operation. Specifically, the postponement of advanced heating, fueling and ash-removal systems from the first-generation power plant, while simultaneously operating with a strong promise of high efficiency and low cost, could lead to a lower-risk approach to fusion power. Once uncertainties are resolved and experience is gained through batch-burn operation, improvement of system performance can be achieved by incorporating fueling and ash-removal systems, leading ultimately to a steady-state power plant. These improvements would be achieved from the stronger technology base and operating experience that could be built from economic, batch-burn operation.

REFERENCES

1. R. L. Hagenson, R. A. Krakowski, and G. E. Cort, "The Reversed-Field Pinch Reactor (RFPR) Concept," Los Alamos Scientific Laboratory report LA-7973-MS (1979).

2. J. B. Taylor, "Relaxation of Toroidal Discharges," Proc. 3rd Topical Conference on Pulsed High Beta Plasmas," Culham, United Kingdom, 59 (1976).

3. A. A. Newton, Li Yin-An, I. W. Lone, and B. G. Young, "Numerical Investigation of Reversed Field Pinches," Proc. 3rd Topical Conference on Pulsed High Beta Plasmas," Culham, United Kingdom, 323 (1976).

4. R. A. Nebel, R. L. Hagenson, R. W. Moses, and R. A. Krakowski, "Comparison of Zero-Dimensional and One-Dimensional Thermonuclear Burn Computations for the Reversed-Field Pinch Reactor (RFPR)," Los Alamos Scientific Laboratory report LA-8185-MS (1980).

5. D. A. Baker and L. N. DiMarco, "The LASL Reversed-Field Pinch Program Plan," Los Alamos Scientific Laboratory report LA-6173-MS (1975).

6. H. A. Bodin, "Reversed Field Pinches," Proc. 3rd Topical Conference on Pulsed High Beta Plasmas," Culham, United Kingdom, 49-57 (1976).

7. S. Ortolani (Scientific Secretary), Proc. Workshop on the Reversed Field Pinch (RFP), Universita de Padova, Padova, Italy (1978).

8. A. Hirose and H. M. Skarsgard, "On the Energy Confinement Times of Tokamaks," Nucl. Fusion, 18, 1737-1742 (1978).

9. A. M. Berlizov, G. V. Bobrovskij, A. A. Bogdanov, V. S. Vasin, A. V. Vertiporokh, and V. P. Vinogradov, "First Results from the T-10 Tokamak," Proc. 6th Conf. on Plasma Physics and Controlled Nucl. Fus. Res., Berchtesgaden, 1, 3-13 (1976).

10. P. Apcar, W. Coppi, A. Gondhalekar, H. Helava, D. Pfirsch, and F. Troyon, "High-Density and Collisional Plasma Regimes in the Alcator Programme," Proc. 6th Conf. on Plasma Physics

and Controlled Nucl. Fus. Res., Berchtesgaden, 1976, 1, 247-266 (1976).

11. R. L. Hagenson and R. A. Krakowski, "A Cost-Constrained Design Point for the Reversed-Field Pinch Reactor," Am. Nucl. Soc. Third Topical Mtg. on the Technology of Cont. Nucl. Fus., Santa Fe, New Mexico, 1, 90-100 (1978).

12. B. C. Young, J. W. Long, and A. A. Newton, "Reactor Burning Calculations for a Model Reversed Field Pinch," Proc. 3rd Topical Conference on Pulsed High Beta Plasmas," Culham, United Kingdom, 575-579 (1975).

13. T. A. Oliphant, G. E. Gryczkowski, and T. Kammash, "Transient Charge-Exchange Effects in a Neutral-Gas Layer," Nucl. Fus. 16, 263-268 (1976).

14. R. Bancox, M. Bogatin, L. J. Baker, S. Bobbio, W. J. Crawley, and P. A. Daveaport, "A 600 MW(e) Reversed Field Pinch Reactor Study," in Fusion Reactor Design Concepts (IAEA Workshop on Fusion Reactor Design, Madison Wisconsin, 1977), IAEA, Vienna 319 (1979) (Also Culham Laboratory report CLM-P 501).

15. R. Bancox and C. R. Walters, "A Reversed Field Pinch with Superconducting Windings," Proc. 7th International Conference on Plasma Physics and Controlled Nuclear Fusion Research, Innsbruck, Austria (1978).

16. P. W. Taubenblat, W. R. Opie, and Y. T. Hsu, "A New Copper Alloy with High Strength and Conductivity," Metals Engineering Quarterly, 39 (1972).

17. B. Badger, R. W. Conn, G. L. Kulcinski, C. W. Maynard, R. Aronstein, and H. I. Avci, "UWMAK-III, A Noncircular Tokamak Power Reactor Design," University of Wisconsin report UWFDM-150 (1976).

18. K. I. Thorsen (ed.), "Conceptual Engineering Design of a One-GJ Fast Discharging Homopolar Machine for the Reference Theta-Pinch Reactor," Electric Power Research Institute report EPRI-ER-246, Project 469 (1976).

19. M. Kristiansen (coordinator), "Proceedings of the Workshop on Switching Requirements and R&D for Fusion Reactors," Electric Power Research Institute Special report EPRI ER-376-SR (1977).

20. Staff of the CTR Division (Compiled by H. Dreicer), "The Reversed Field Pinch Concept and a Preliminary Conceptual Design for a Proof-of-Principle Experiment," Los Alamos Scientific Laboratory report LA-7527-MS (1979).

21. D. Weldon and J. Wollen, personal communication, Los Alamos Scientific Laboratory (1978).